Supporting Information

Experimental section

Preparation for ZIF-67

Typically, $Co(NO_3)_2 \cdot 6H_2O$ (0.22 g) was dissolved in 9 mL of deionized (DI) water, then 2-methylimidazole (0.052 g) in 9 mL of methanol was added into above solution under vigorously stirred for 5 min at room temperature. The resulting purple precipitates were collected by centrifuging, washed with methanol for one times, and finally dried in vacuum at 50 °C overnight.

Preparation for Ag NWs-ZIF67 composites

1D Ag NWs were prepared based on the previous report.[13] The products at the bottom were simply centrifuged and Ag NWs with high quality were obtained. The as-obtained Ag NWs were dispersed in methanol, and the concentration was kept at 3.3 mg mL^{-1}. The Ag NWs-ZIF67 composite was prepared by in situ growth. In a typical experiment, 18 mL Ag NWs solution (methanol: deionized water = 1: 1) was firstly sonicated for 5 min, and then $Co(NO_3)_2 \cdot 6H_2O$ (0.22 g) and 2-methylimidazole (0.052 g) were slowly added into the above solution with fully magnetic stirring. After thorough stirring for 5 min, the as-obtained precipitates were centrifuged and washed with methanol for one times, and finally dried in vacuum at 50 °C overnight.

Materials Characterization

XRD measurement was performed on examined on a Bruker D8 Advanced X-ray diffractometer (Cu Kα radiation: λ = 0.15406 nm) with scanning angle 2θ ranging from 10° to

80°. XPS were recorded on an ESCAL AB250 system with monochromatic Al Kα excitation Q3 under vacuum better than 1×10^{-7} Pa. The binding energy (BE) is calibrated with C 1s = 284.6 eV. SEM images were investigated by Zeiss-Supra 55. TEM images were obtained by Tecnai G2 F30 S-TWIN.

Electrochemical catalysis

A standard three-electrode glass cell equipped with a Pt wire counter electrode and an Hg/HgO reference electrode was employed for electrochemical characterizations. The three-electrode system was used for OER, ORR performance, durability and impedance measurements. The measurements were performed in 0.1 M KOH aqueous electrolyte at room temperature. The working electrode should be polished mechanically with Al_2O_3 powders (Aldrich, 0.05 mm) to receive a mirror-like surface and washed with the ethanol and deionized water and then dried in air. The catalyst film coated glass carbon electrode (GCE, diameter: 3 mm) or rotating-disk electrode (RDE, disk diameter: 5 mm) were used for OER and ORR measurements, respectively. Subsequently, 0.5 wt% Nafion (120 μL) and catalyst (5 mg) were dissolved in 1 mL mixed solvent containing 1:2 v/v water/ethanol for more than 30 min sonication to produce a homogeneous ink. Then 2.83 μL catalyst ink (0.0142 mg catalyst) was dropped onto the GCE (~ 0.2 mg cm^{-2}). The electrode was dried under room temperature before trying to use it. Before OER measurements, the electrode was pretreated with 20 cycles of CV at the range of 1.0-1.6 V (vs RHE) for the electroactivation to increase OER catalytic species. The OER performances were measured at the range of 1.2-1.7 V (vs RHE) by the LSV method at 5 mV s^{-1}. The ORR activities were conducted in an oxygen-saturated KOH (0.1 M) aqueous electrolyte with the rotation speed of 300, 600, 900, 1200, 1600, 2000 and

2500 rpm. The polarization curves for ZIF-67, Ag NWs, Ag NWs-ZIF67 composite and Pt/C catalysts were obtained at 5 mV s^{-1}.

The electron transfer number *n* is determined by following equation:

$$n = \frac{1}{0.62\kappa F {D_0}^{2/3} \nu^{-1/6} C_0}$$

(6)

where *k* is the fitted slope from Koutechky-Levich polts, *F* is the Faraday's constant, D_0 is the O_2 diffusion coefficient of in 0.1 M KOH (1.93×10^{-5} $cm^2\cdot s^{-1}$), *v* is the kinematic viscosity of the electrolyte (1.09×10^{-2} $cm^2\cdot s^{-1}$) and C_0 is the saturation concentration of O_2 in 0.1 M KOH at 1atm O_2 pressure (1.26×10^{-6} $mol\cdot cm^{-3}$). The durability tests for catalyst were carried out by 500, 1000, 5000 times CV cycles at 100 mV s^{-1}, and the LSVs were measured after cycling. E(Hg/HgO) is electrode potential of KOH-saturated Hg/HgO reference electrode (0.205 V vs. SHE). RHE calibration was carried out before each characterization in a hydrogen-saturated 0.1 M KOH electrolyte using a Pt RDE as working electrode. The measured current densities were normalized to surface area of GC electrode and measured potentials vs. Hg/HgO electrode were converted to a RHE scale on the basis of the Nernst equation (7).

$$E_{RHE} = E_{Hg/HgO} + E^{\Theta}_{Hg/HgO} + 0.059 \times pH$$

(7)

The overpotentials (η) of OER were obtained from

$$\eta OER = E(RHE) - 1.23 \text{ V} \quad (8)$$

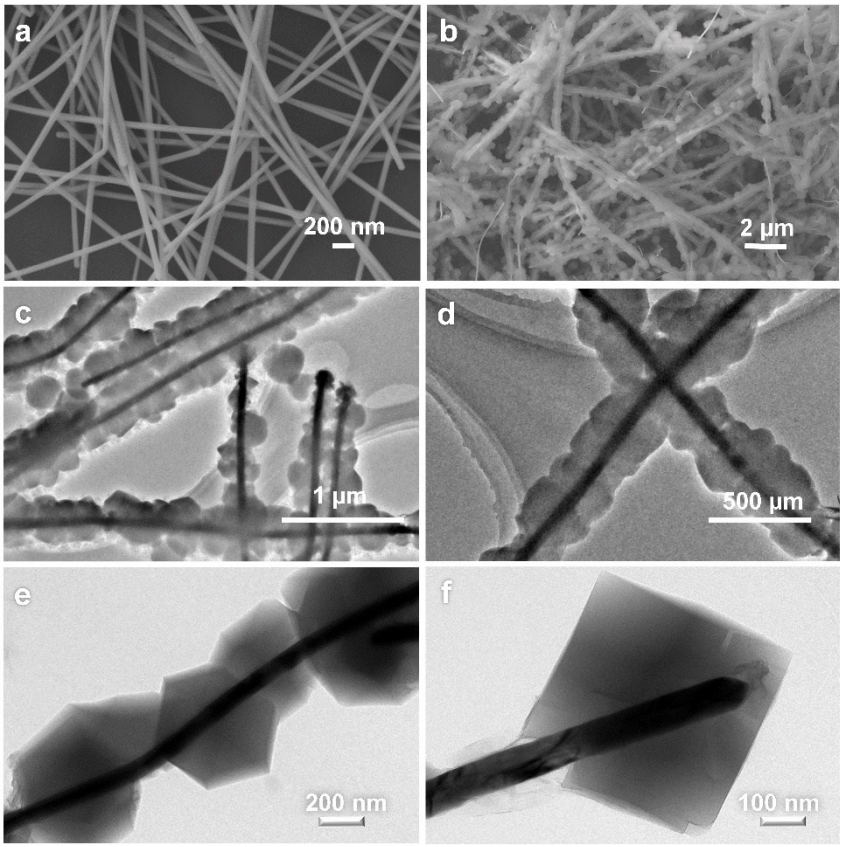

Figure S1. SEM image of (a) Ag NWs, and (b) the Ag NWs-ZIF67 composite, (c-f) TEM images of the Ag NWs-ZIF67 composite.

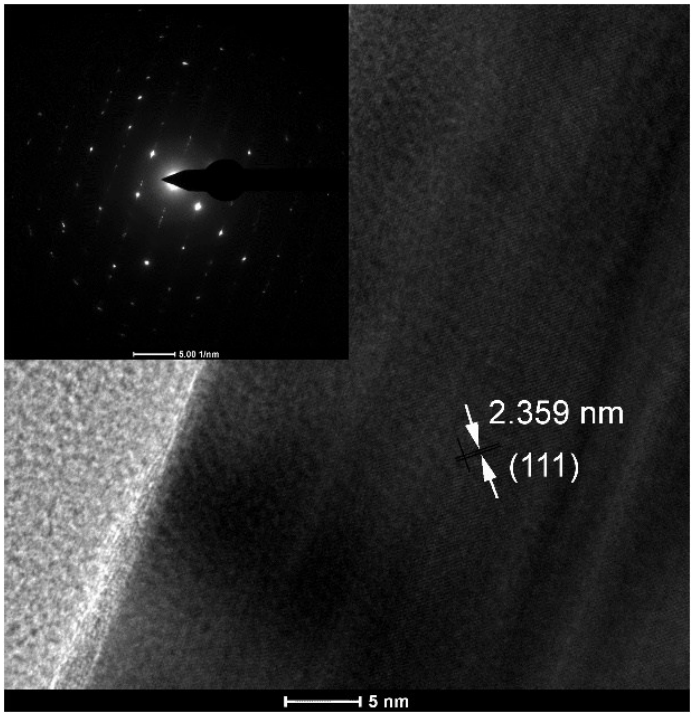

Figure S2. HRTEM images of Ag NWs (inset: SAED pattern of Ag NWs).

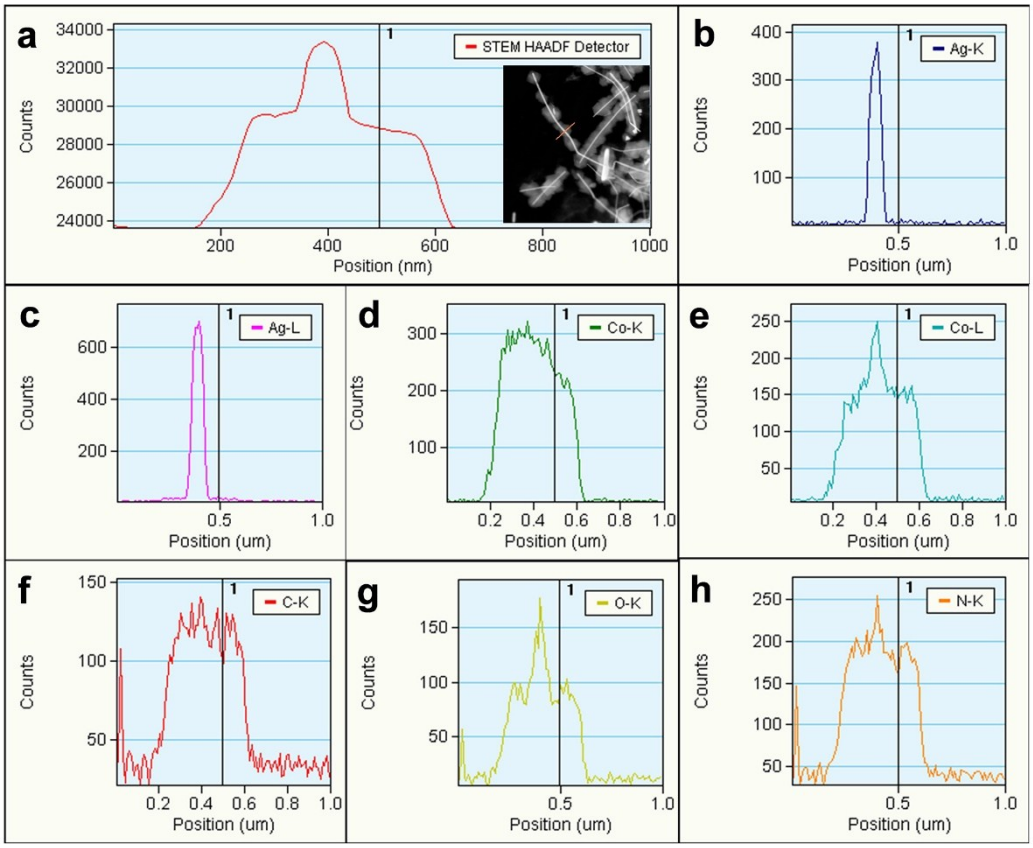

Figure S3. EDS line scanning of (a) STEM HAADF Detector (inset: TEM image), (b, c) Ag, (d, e) Co, (f) C, (g) O, and (h) N.

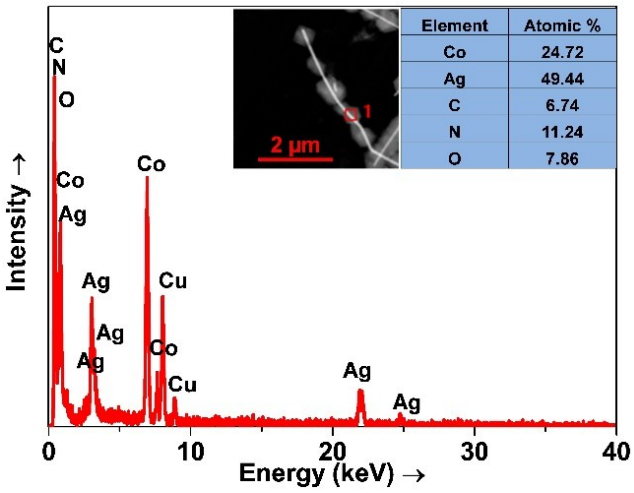

Figure S4. EDS spectra of the Ag NWs-ZIF67 composite. The insets show the TEM and the corresponding atomic ratio of the products.

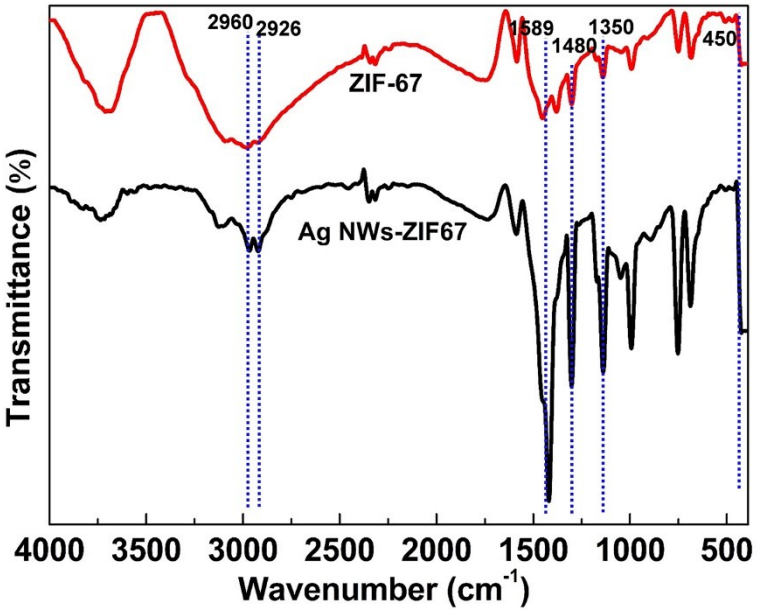

Figure S5. FTIR spectra of ZIF-67 and the Ag NWs-ZIF67 composite.

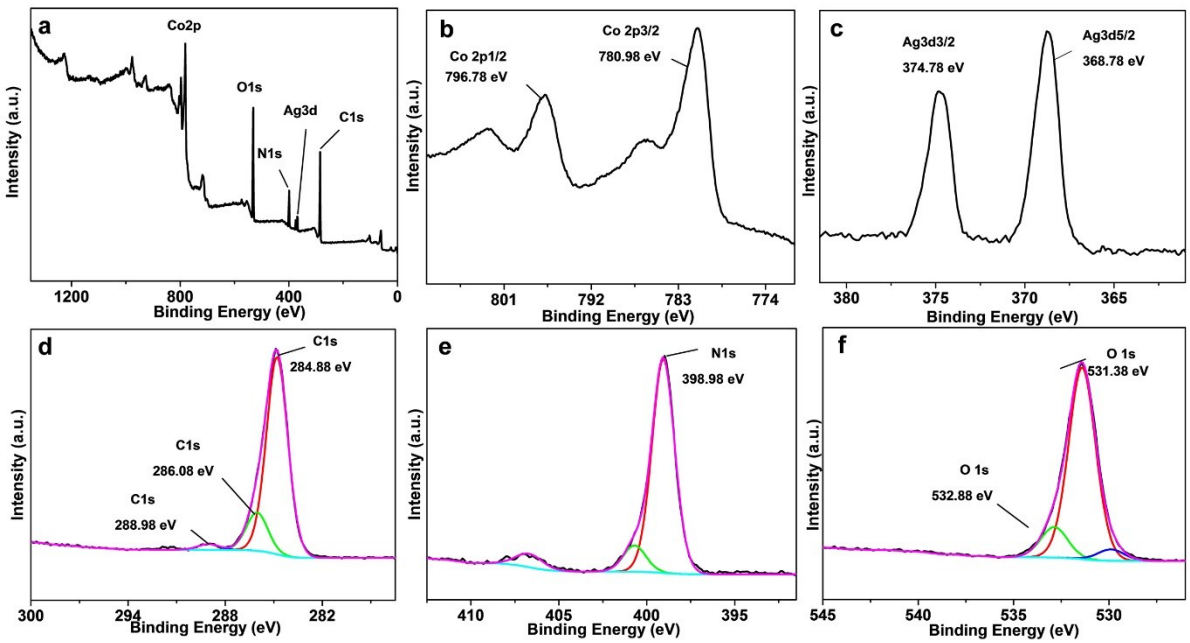

Figure S6. XPS (a: survey, b: Co 2p, c: Ag 3d, d: C 1s, e: N 1s, f: O 1s) spectra for the Ag NWs-ZIF67 composite.

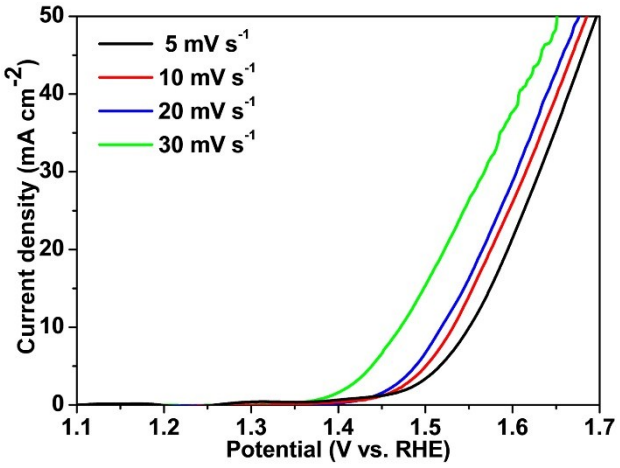

Figure S7. OER polarization curves of the Ag NWs-ZIF67 composite at different scan rates.

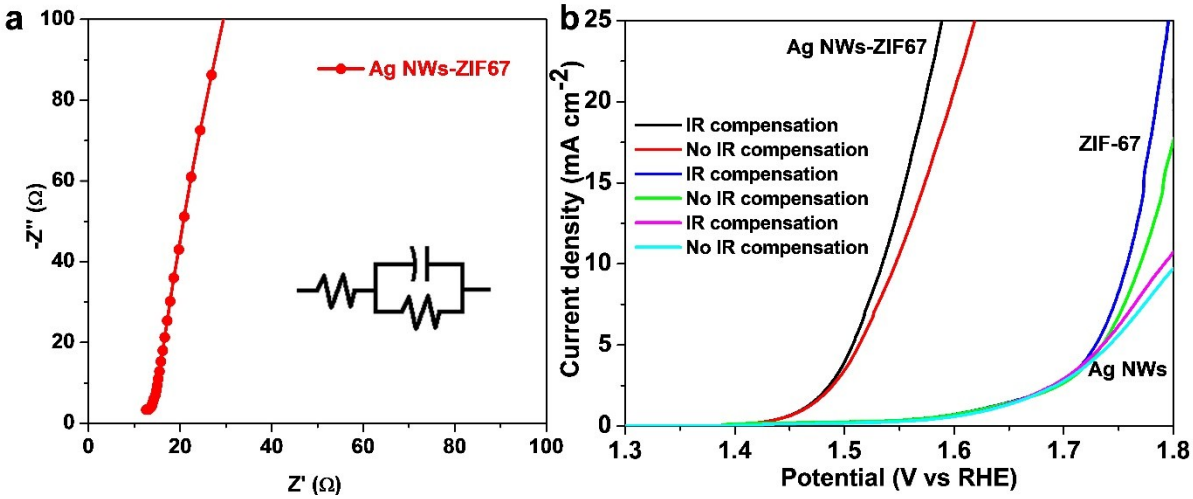

Figure S8. a) The electrochemical impedance spectra measured at open circuit potential in 0.1 M KOH at pH = 13 was fitted by the inset circuit to give R_u = 17 Ω, which was then used to adjust IR compensation. b) The IR-corrected OER activity curves of Ag NWs-ZIF67, ZIF-67 and Ag NWs. The potentials were adjusted to compensate for the Ohmic potential drop losses (R_u) that arose from the solution resistance and calibrated with respect to the reversible hydrogen electrode (RHE), in which Evs.RHE = Evs.Hg/HgO + 0.098 + 0.05916 pH - I×R_u. The IR (I × R) compensation was done by the method of positive feedback, and the compensation level is 95%.

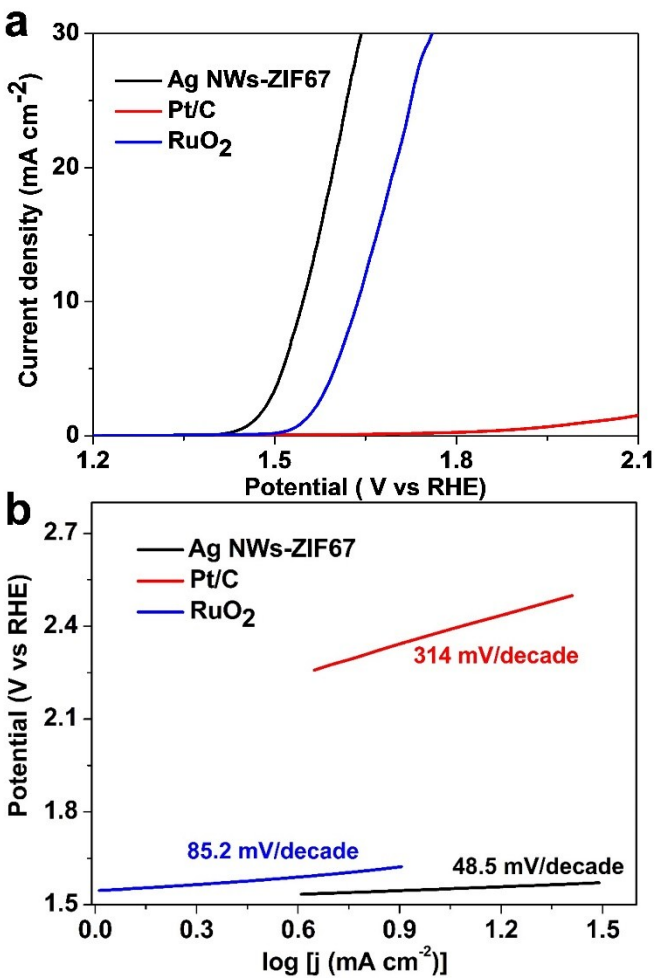

Figure S9. a) The polarization curves of the Ag NWs-ZIF67 composite, Pt/C, and RuO_2 at a scan rate of 5 mV s^{-1} in 0.1 M KOH. b) Corresponding Tafel plots obtained from the polarization curves.

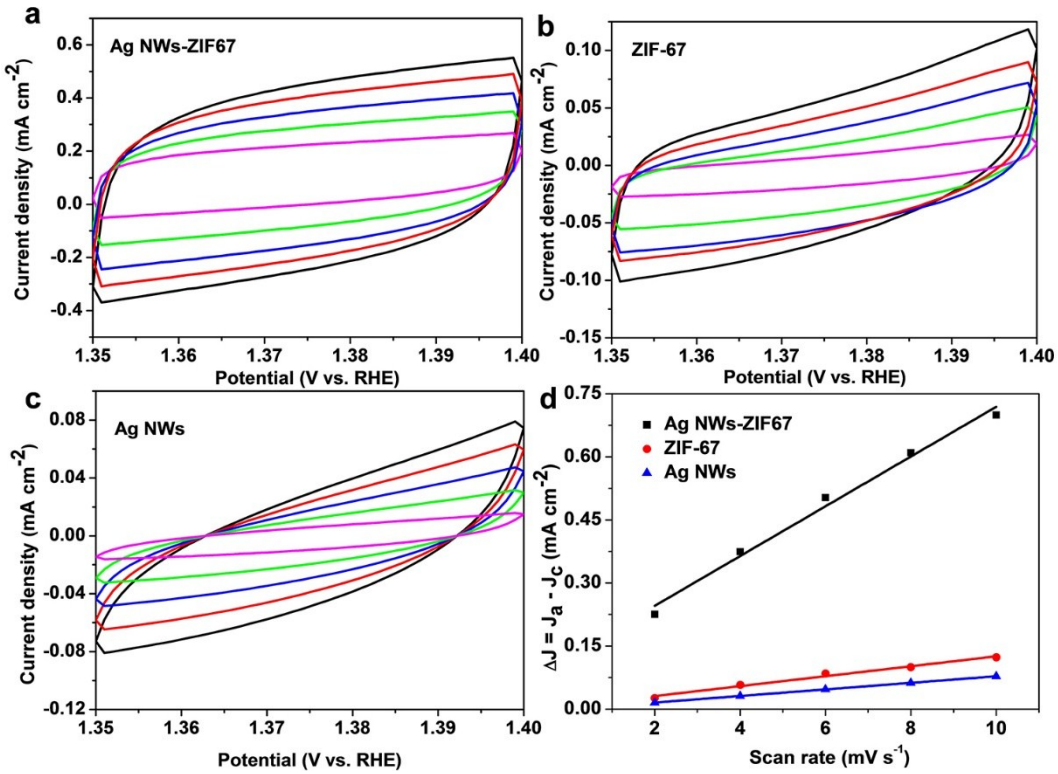

Figure S10. CV of the Ag NWs-ZIF67 composite (a), ZIF-67 (b), and Ag NWs (c) (Potential from 1.35 V to 1.40 V) measured in 0.1 M KOH at scan rates of 2-10 mV s^{-1}. (d) Plots of the current density at 1.375 V vs. the scan rate to determine the double layer capacitance (C_{dl}). The C_{dl} of the as-synthesized electrocatalysts were evaluated based on CVs. The CVs of the Ag NWs-ZIF67 composite, ZIF-67 and Ag NWs were recorded at different scan rates (2-10 mV s^{-1}) in a potential region of 1.35-1.40 V (ΔE = 50 mV). The charge transfer electrode reaction is considered as negligible in this voltage range. The current is entirely derived from charging and discharging of electrical double layer. There is a linear relationship between current density (at 1.375 V) and potential scan rate (Figure S6d), and their slope is twice of C_{dl} (C_{dl} of the Ag NWs-ZIF67: 29.6 mF cm^{-2}; C_{dl} of ZIF-67: 5.9 mF cm^{-2}; C_{dl} of Ag NWs: 3.9 mF cm^{-2}).

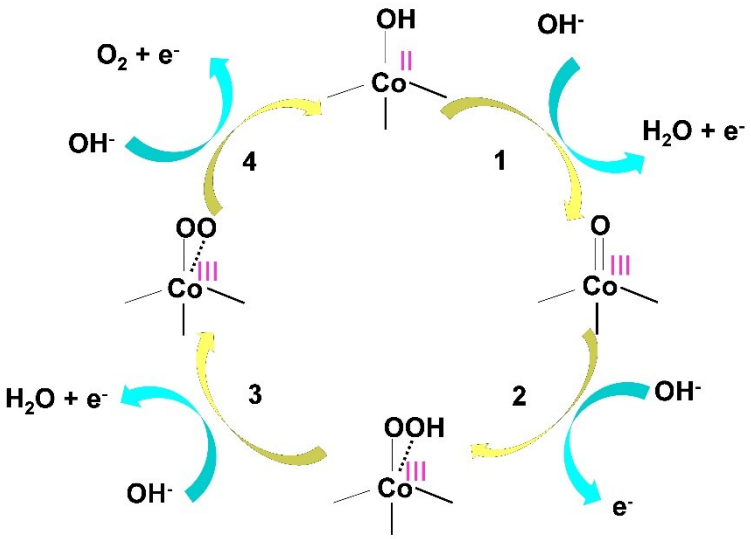

Figure S11. Scheme of the proposed OER mechanism on the Ag NWs-ZIF67 composite.[13] The Roman numerals are the oxidation states of the Co atoms. A reaction circle contains four electron transfer steps.

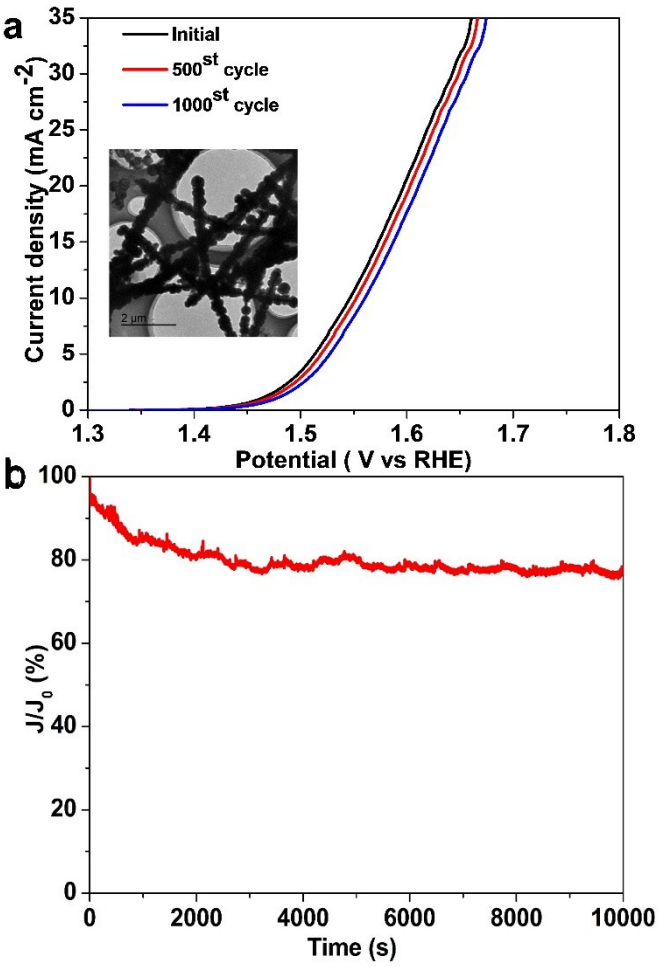

Figure S12. (a) Durability test for the Ag NWs-ZIF67 composite after 1, 500, 1000 cycles (Inset: the TEM image of the Ag NWs-ZIF67 composite after the stability test). (b) Chronoamperometric response at 1.5 V of the Ag NWs-ZIF67 composite in an Ar-saturated 0.1 M KOH solution.

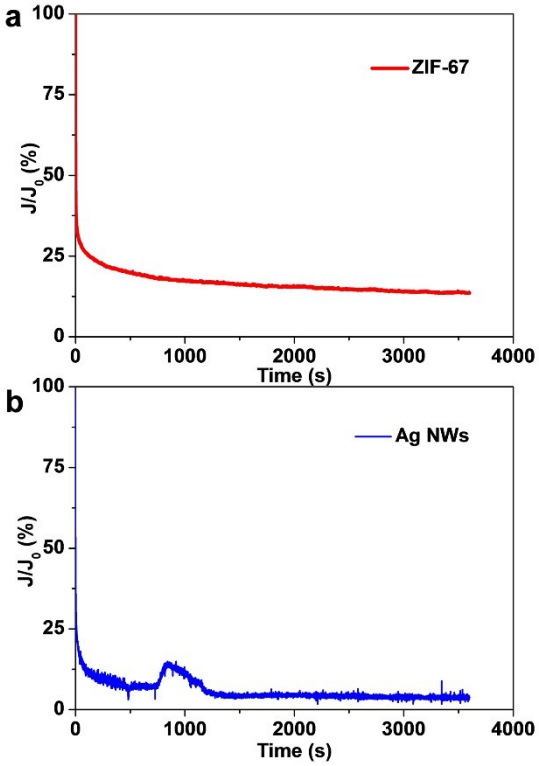

Figure S13. Chronoamperometric response at 1.5 V of a) ZIF-67, b) Ag NWs at 0.1 M KOH solution.

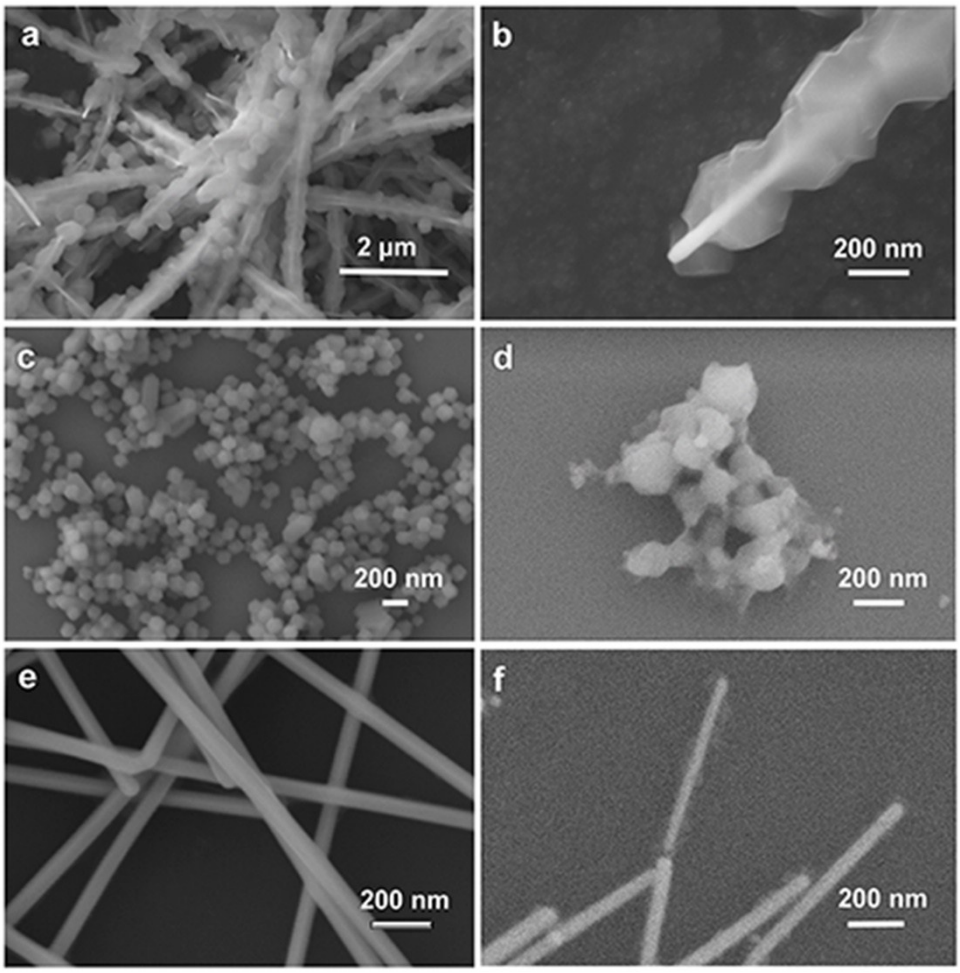

Figure S14. SEM images of Ag NWs-ZIF67 a), ZIF-67 c), Ag NWs e) and Ag NWs-ZIF67 b), ZIF-67 d), Ag NWs f) for OER before and after the stability test.

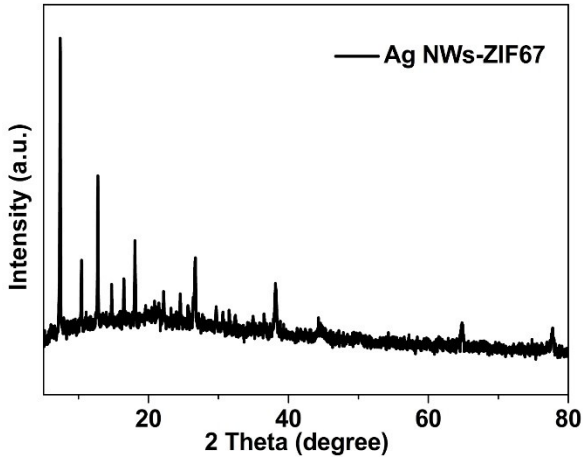

Figure S15. XRD patterns of the Ag NWs-ZIF67 composite after the stability test.

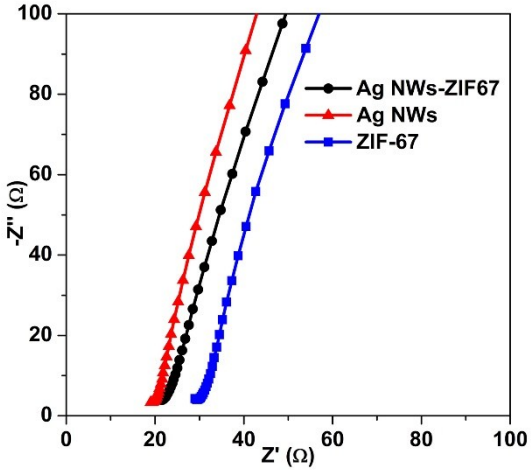

Figure S16. Nyquist plots of the Ag NWs-ZIF67 composite, Ag NWs and ZIF-67 for OER after stability test. The Rct of Ag NWs, the Ag NWs-ZIF67 composite and ZIF-67 are calculated as 19 Ω, 21 Ω and 32 Ω, respectively.

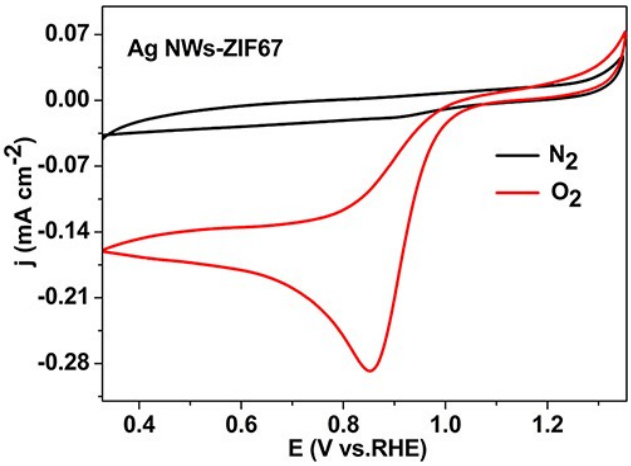

Figure S17. CV curves of the Ag NWs-ZIF67 in N_2 or O_2 saturated 0.1 M KOH solution at a scan rate of 10 mV s^{-1}.

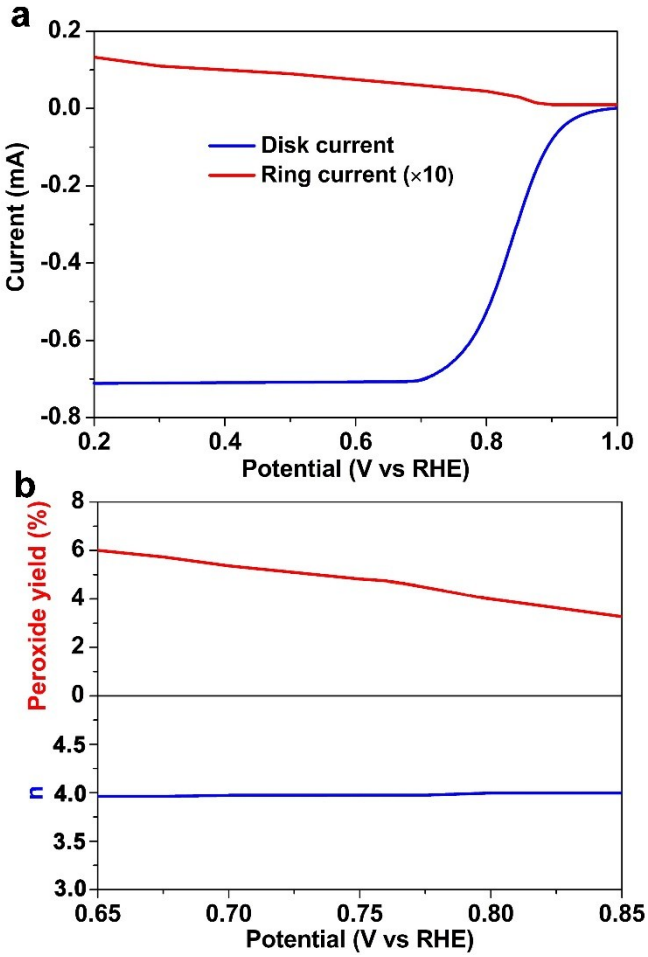

Figure S18. a) RRDE curves of the Ag NWs-ZIF67 composite catalyst in O_2-saturated 0.1 M KOH solution (scan rate: 5 mV s^{-1}; rotation rate: 1600 rpm). The ring potential was constant at 1.3 V versus RHE. b) Peroxide yield (%) and electron transfer number (n) on Ag NWs-ZIF67 at various potentials based on the corresponding RRDE data.

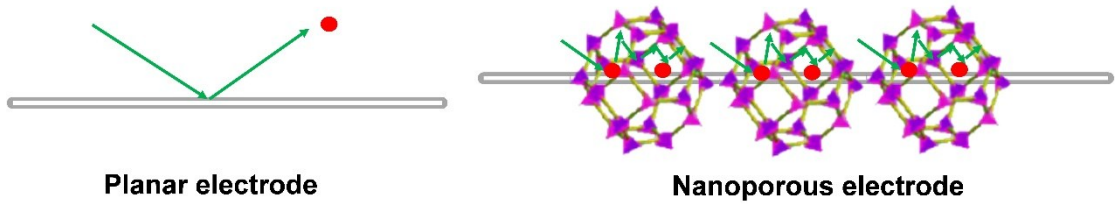

Figure S19. Scheme of proposed ORR mechanism on Ag NWs-ZIF67 composites.

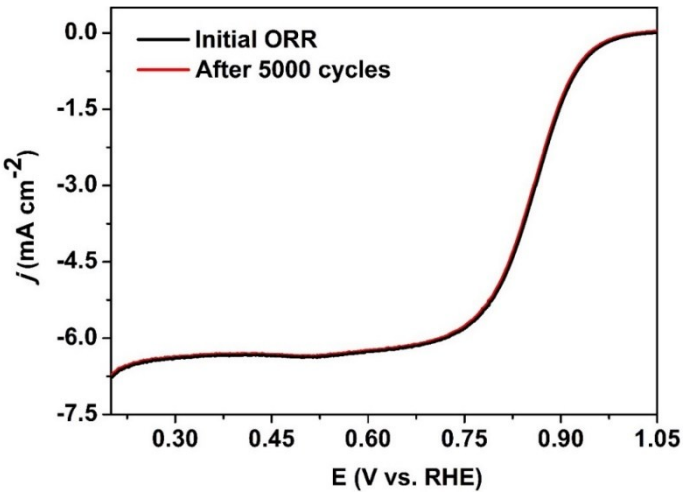

Figure S20. ORR polarization curves of the Ag NWs-ZIF67 composite before and after 5000 cycles.

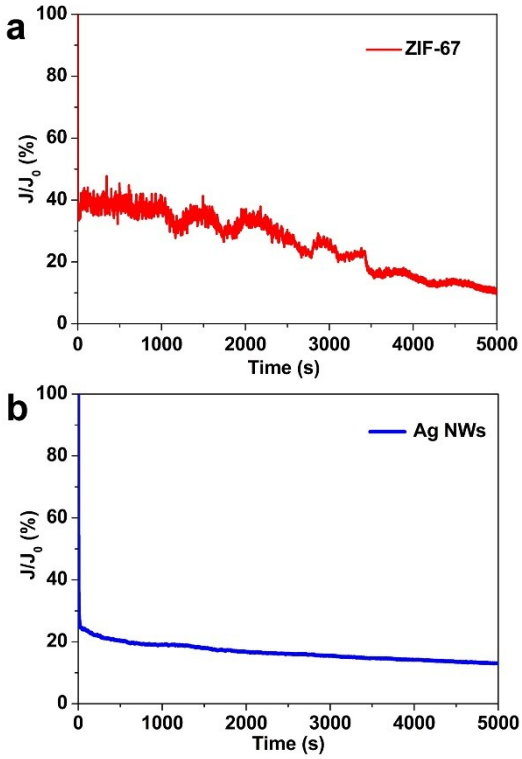

Figure S21. Chronoamperometric response at 0.5 V of a) ZIF-67, b) Ag NWs in the O^{2-} saturated 0.1 M KOH solution.

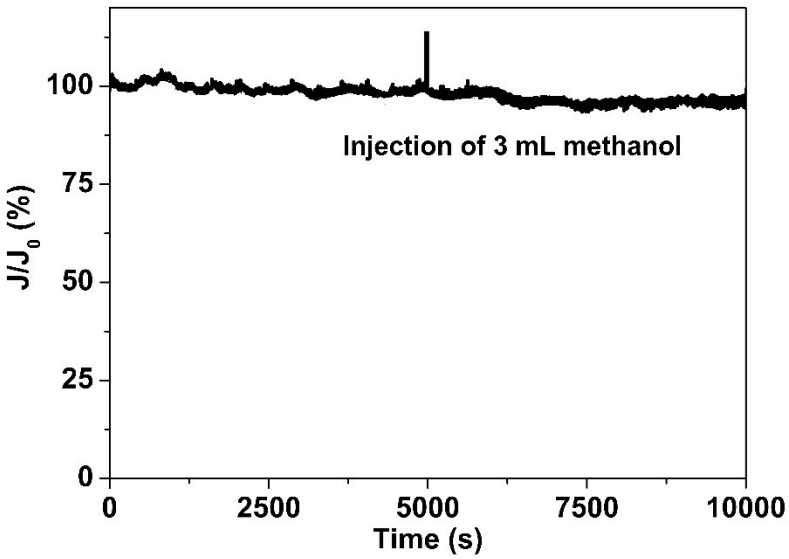

Figure S22. Methanol crossover tests were conducted by injecting 3 mL of methanol into test cells after 10,000 s for the Ag NWs-ZIF67.

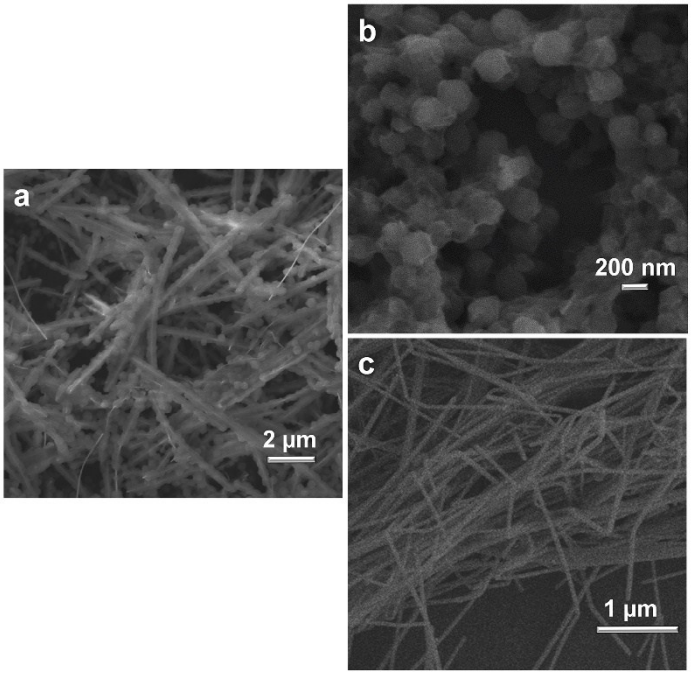

Figure S23. The SEM image of the Ag NWs-ZIF67 a), ZIF-67 b), Ag NWs c) for ORR after the stability test.

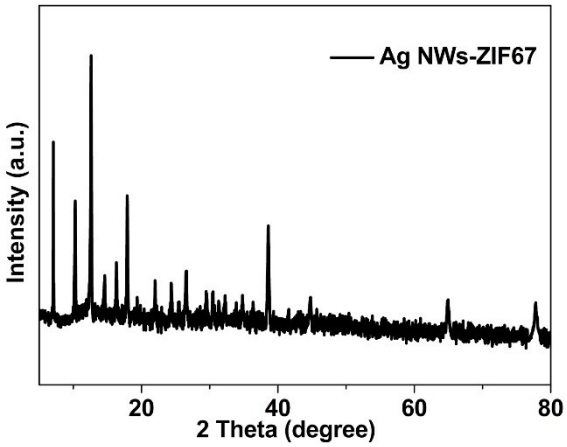

Figure S24. XRD patterns of the Ag NWs-ZIF67 after the stability test.

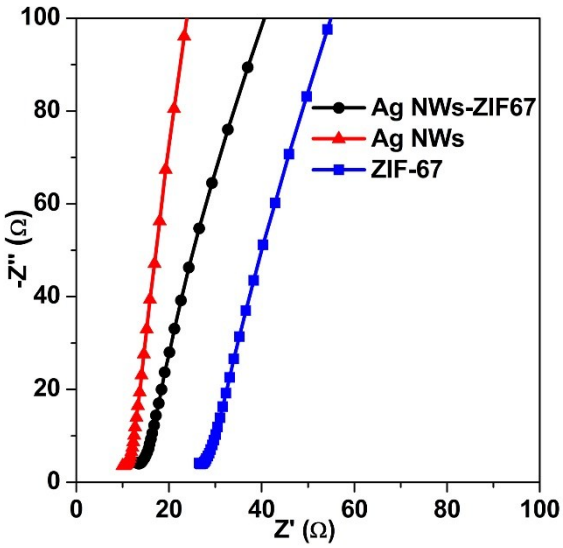

Figure S25. Nyquist plots of the Ag NWs-ZIF67, Ag NWs and ZIF-67 for ORR after stability test. The Rct of Ag NWs, the Ag NWs-ZIF67 and ZIF-67 are calculated as 13 Ω, 15 Ω and 30 Ω, respectively.

Table S1. Comparison of the OER catalytic performance of the Ag NWs-ZIF67 composite with other catalysts.

Catalysts	η versus RHE [V] at 10 mA cm^{-2}	Tafel slope [mV dec^{-1}]	Solution	Ref no.
Ag NWs-ZIF67	**0.316**	**48.5**	**0.1 M KOH**	**This work**
CoS-$Co(OH)_2$@aMoS_{2+x}/NF[a)]	0.38	68	1 M KOH	1
NiS-$Ni(OH)_2$@aMoS_{2+x}/NF	0.417	97	1 M KOH	1
Ti@TiO_2/CdS/ZIF-67	0.41	42	1 M NaOH	2
Co_4N/CNW[b)]/CC[c)]	0.31	81	1 M KOH	3
Co_4N NW/CC	0.257	44	1 M KOH	4

[a)] aMoS_{2+x}/NF: amorphous MoS_{2+x}/Ni foam, [b)]CNW: carbon fibers network, [c)]CC: carbon cloth.

Table S2. Comparison of the ORR catalytic performance of the Ag NWs-ZIF67 composite with other catalysts composed of Ag and Co.

Catalysts	Oneset potential (V vs RHE)	Limiting current density (mA cm^{-2})	n value	Solution	Ref no.
Ag NWs-ZIF67	**0.038[b]**	**-6.74[b]**	**3.85-3.98**	**0.1 M KOH**	**This work**
AgCo nanotubes	-0.067[b]	-4.75[b]	3.80	0.1 M NaOH	5
Carbon-supported Ag-Co NPs	ca. -0.09[a]	-5.41[c]	3.92-4.03	0.1 M NaOH	6
Ag/Co_3O_4-C	-0.1[a]	-2.39[b]	3.8-4.0	1 M KOH	7
Ag-Co/C	-0.11[a]	-3.0[b]	3.0	1 M KOH	8
Cobalt monolayer on Ag (111)	-0.14[a]	-2.75[d]	2.9-3.0	0.1 M KOH	9
P-CNCo-20	-0.04[b]	-6.0[b]	2.3-3.9	0.1 M KOH	10
Co,N-CNF	-0.082[b]	-5.71[b]	unknown	0.1 M KOH	11

[a]Potentials are converted to the values vs SCE. [b]At 1600 rpm. [c]At 900 rpm. [d]At 500 rpm.

Reference

1 T. Yoon and K. S. Kim, *Adv. Funct. Mater.*, 2016, **26**, 7386.

2 T. Zhang, J. Du, H. L. Zhang and C. L. Xu, *Electrochimi. Acta*, 2016, **219**, 623.

3 F. L. Meng, H. X. Zhong, D. Bao, J. M. Yan and X. B. Zhang, *J. Am. Chem. Soc.*, 2016, **138**, 10226.

4 Z. Chen, K. Xu, Z. W. Fang, Y. Tong, J. C. Wu, X. L. Lu, X. Peng, H. Ding, C. Z. Wu and Y. Xie, *Angew. Chem. Int. Ed.*, 2015, **54**, 14710.

5 A. Yu, C. Lee, N. S. Lee, M. H. Kim and Y. Lee, *ACS Appl. Mater. Interfaces*, 2016, **8**, 32833.

6 L. Zeng, T. S. Zhao and L. An, *J. Mater. Chem. A*, 2015, **3**, 1410.

7 P. Singh and D. A. Buttry, *J. Phys. Chem. C*, 2012, **116**, 10656.

8 Y. Wang, X. Lu, Y. Liu and Y. Deng, *Electrochem. Commun.*, 2013, **31**, 108.

9 S. He, J. Yao, S. Xie, S. Pang and H. Gao, *Chem. Phys. Lett.*, 2001, **343**, 28.

10 Y. Z. Chen, C. M. Wang, Z. Y. Wu, Y. J. Xiong, Q. Xu, S. H. Yu and H. L. Jiang, *Adv. Mater.*, 2015, **27**, 5010.

Lu

Shang ,

Huijun Yu, Xing Huang, Tong Bian,

Run Shi, Yufei Zhao, Geoffrey I.

N. Waterhouse Li-Zhu Wu, Chen-Ho Tung,

and Tierui Zhang

11 L. Shang, H. J. Yu, X. Huang, T. Bian, R. Shi, Y. F. Zhao, G. I. N. Waterhouse, L. Z. Wu, C. H. Tung and T. R. Zhang, *Adv. Mater.*, 2016, **28**, 1668.

12 N. T. Suen, S. F. Hung, Q. Quan, N. Zhang, Y. J. Xu and H. M. Chen, *Chem. Soc. Rev.*, 2017, **46**, 337.

13 Z. B. Zhuang, W. C. Sheng and Y. S. Yan, *Adv. Mater.*, 2014, **26**, 3950.

14 T. Cheng, Y. Z. Zhang, W. Y. Lai, Y. Chen, W. J. Zeng and W. Huang, *J. Mater. Chem. C*, 2014, **2**, 10369.